STRENGTHENING MECHANISMS IN AN Al-0.9Mg-0.2Zr (wt.%)ALLOY AFTER ISOTHERMAL AGING

Pedro Henrique Lamarão Souza, pedro.lamarao@posgrad.ufsc.br[1]
Carlos Augusto Silva de Oliveira, carlos.a@ufsc.br[2]
José Maria do Vale Quaresma, quaresma@fem.unicamp.br[2]

[1]Universidade Federal de Santa Catarina – UFSC, Campus Universitário João David Ferreira Lima, rua Delfino Conti, s/n, Trindade, Florianópolis – SC, CEP: 88040-900
[2]Universidade Federal do Pará – UFPA, Campus Guamá, rua Augusto Corrêa, nº 01, Guamá, Belém – PA, CP.479, CEP: 66075-110

Abstract. *The present work quantifies the active strengthening mechanisms due to solid solution and precipitation hardening in an Al-0.9Mg-0.2Zr (wt.%) alloy, using literature models, microstructural characterization with a Transmission Electron Microscope – TEM and Vickers microhardness tests. The studied alloy was conventionally cast and isothermally aged at the temperature of 650 or 700 K (377 or 427 ºC) for 4, 12, 24, 100 and 400 h. The microhardness of the as-cast samples presented an increase of 136 MPa (13.9 HV 0.2), attributable to solid solution strengthening from Mg, comparing to an Al-0.2Zr alloy. Samples aged at 650 K presented an increase in strength after 24 h of aging and peak-strength after 100 h, while after 400 h it presented the same microhardness of the as-cast samples. During aging at 700 K no significant increase in strength was observed. Nanometer-scale Al_3Zr, with a mean radius of 8 nm, and β-Al_3Mg_2, with a mean radius of 235 nm were identified in the microstructure of the alloy. Comparing the increase in strength due to the studied mechanisms, one obtained good agreement between the experimental and theoretical results.*

Keywords: *Al alloys, precipitation hardening, solid solution hardening, strengthening mechanisms.*

1. INTRODUCTION

Al-Zr alloys have emerged as a promising system for high temperature applications (Kumar, 1990); (Knipling et al., 2006); (Knipling et al., 2007). During artificial aging, nanometer-scale fcc Al_3Zr precipitates, promote hardening in the alloy. These are coherent with the Al matrix, presenting a precipitate/matrix mismatch of 0.75% (Knipling et al., 2006), and high thermal stability after aging at elevated temperatures for prolonged times (Zedalis and Fine, 1986), comparing with other Al_3X-based Al alloys (X = Sc, Er, or Hf) (Marquis et al., 2003); (Zhang et al., 2014); (Wu et al., 2014).

Mg additions to Al are often employed to promote solid solution hardening in cold worked alloys in the 5XXX series, due to its capability of increasing work hardening (Sanders et al., 1989). In the 6XXX and 7XXX alloy series, Mg is combined with Si and Zn, respectively, to form Mg_2Si and $MgZn_2$ precipitates during heat-treating(Hatch, 1984).

Few studies focused on the synergetic effect of solid solution additions and precipitation hardening in Al-Mg-Zr alloys. Kendig and Miracle (2002) quantified the strengthening mechanisms in an Al-6Mg-2Sc-1Zr (wt.%) alloy prepared by powder metallurgy and extruded at 623 K (350 ºC). The authors obtained reasonable agreement between the experimental and theoretical results, and second-particle strengthening was obtained by the nanometer-scale $Al_3(Sc,Zr)$ with a mean precipitate radius - $\langle r \rangle$ = 7.5 nm. Robson and Prangnell (2003) performed simulations of the effect of Cu, Mg and Zn solid solutions to the precipitation kinetics of Al_3Zr dispersoids. The authors showed that Mg additions had the greater effect in increasing the precipitate number density and in reducing its radius, but no information about the mechanical properties of the material was given.

The present work studied the solid solution and precipitation hardening mechanisms in a conventionally cast and artificially aged Al-0.9Mg-0.2Zr (wt.%) alloy, quantifying such mechanisms using literature models, information from its microstructural characterization and comparing it with experimental results.

2. MATERIALS AND METHODS

The materials used for alloy preparation were: high purity Al ingots (Al ≥ 99.8 %), Al-10%Zr waffles and Mg ingots (99.8 %), all compositions in weight %. After careful preparation of the correct proportions of each material, the Al ingot and alloying elements were inserted in a pre-heated SiC crucible, previously coated with kaolin, to avoid heat loss. The crucible was inserted in a muffle furnace and hold at 1120 K (847 ºC) for 40 minutes, to guarantee fusion of the materials. Subsequently, the crucible was removed from the furnace. The melt was stirred to promote homogenization of the liquid, and degassed using inert gas (Ar). The alloy was monitored using K type thermocouples and an ALMEMO data logger. After reaching a temperature of 1052 K (± 1 K) (779 ºC), the alloy was poured in a water-cooled Cu mold, to guarantee fast heat extraction.

The produced ingot had a mass of ~ 600 g and was sectioned using a cut-of machine, producing 10 mm cubic samples. These were aged in a muffle furnace at 650 K (377 ºC) or 700 K (427 ºC), for 4, 12, 24, 100 and 400 h. After heat-treatment, the materials were quenched in room-temperature water.

The chemical analysis of the produced alloy was obtained in a BRUKER Q4 TASMAN Optical Mass Spectrometer and is shown in Table 1.

Table 1. Chemical composition of the produced alloy (in wt.%).

Alloy	Mg	Zr	Fe	Si	Others	Al
Al-0.9Mg-0.2Zr	0.91	0.19	0.10	0.04	0.05	98.71

After aging, samples were metallographically prepared to Vickers microhardness tests, which were performed using a 1.96 N (200 gf) load and 5 s of dwelling time. Microstructural analysis was carried out using a JEOL JEM 1011 Transmission Electron Microscope, with 100 kV of accelerating voltage, employing bright-field, dark-field and Selected Area Diffraction Pattern – SADP techniques. TEM foil samples were prepared by grinding to 100 µm thickness and electropolishing in a STRUERS TENUPOL 5 twin jet machine, using an electrolyte of 1/3 nitric acid and 2/3 methanol. The precipitate mean radius – $\langle r \rangle$ of the alloys was measured using 4 samples for each kind of precipitate, with a total of 100 particles counted. Measurements were performed using ImageJ software.

3. RESULTS AND DISCUSSION

3.1. Age hardening

Figure 1 shows microhardness results of the studied alloy, where t is the aging time. At the as cast condition, its value is 39.6 HV 0.2 (388 MPa, using a conversion factor from Knipling (2006)), indicating that there is hardening due to Mg solid solution, once the as-cast microhardness of an Al-0.20Zr alloy was also tested, resulting in the value of 25.7HV0.2 (252 MPa). In the second y axis results were transformed to MPa using a conversion chart (Knipling, 2006).

During aging at 650 K, microhardness values presented an increase after 24 h of heat-treatment, reaching a peak-strength of 47.1 HV 0.2 (462 MPa) after 100 h and overaging at 400 h, were microhardness values decreased to the as-cast level. During aging at 700 K, no significant increase in strength was observed in the range of 4 - 400 h.

Following other study in the literature (Knipling et al., 2007), dilute Al-0.34Zr alloys artificially aged typically present peak-microhardness values between 24 – 100 h of aging, with small variation in this time range. Also, even after aging at 647 K (375 ºC) for 400 h, Al-0.34Zr and Al-0.67Zr alloys present little variation in microhardness, comparatively to its peak-values, differently of what is observed in Fig.1.

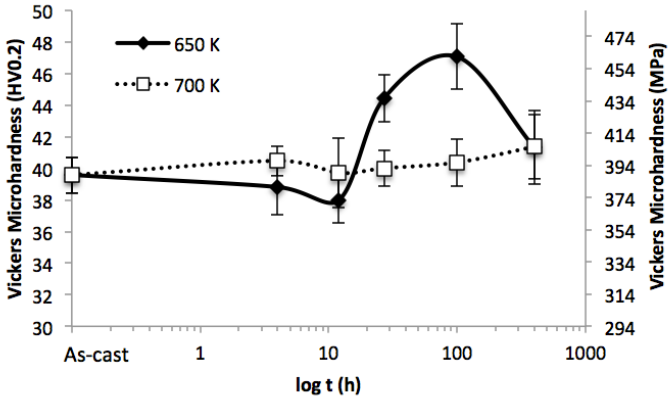

Figure 1. Vickers microhardness of the Al-0.9Mg-0.2Zr alloy isothermally aged as a function of the log of aging time for the studied temperatures.

3.2. Microstructural analysis

Figure 2 presents bright-field TEM micrographs of the Al-0.9Mg-0.2Zr alloy aged at 650 K for 100 h. In Fig.2a it is possible to observe nanometer-scale spherical precipitates and in Fig. 2b is its SADP, which shows evidence of Al_3Zr particles with $L1_2$ structure (ordered fcc), due to the presence of, weaker, superlattice reflections, such as (1-10). Fig. 2c is a micrograph with greater magnification, exhibiting Al_3Zr particles, with $\langle r \rangle$ = 8 ± 1 nm. Fig.2d shows another kind of precipitate, the micrometer-scale β, with $\langle r \rangle$ = 235 ± 77 nm. In Fig.2d, the largest particles are along a grain

boundary (which is indicated by an arrow). The SADP in Fig.2d presents (444) and (777) planes, that suggest the presence of the cubic β-Al_3Mg_2 Samson phase. The work of Kendig and Miracle (2002) and Marquis et al. (2003), which studied Al-6Mg-2Sc-1Zr and Al-2Mg-0.2Sc alloys, respectively, showed no evidence of such structure.

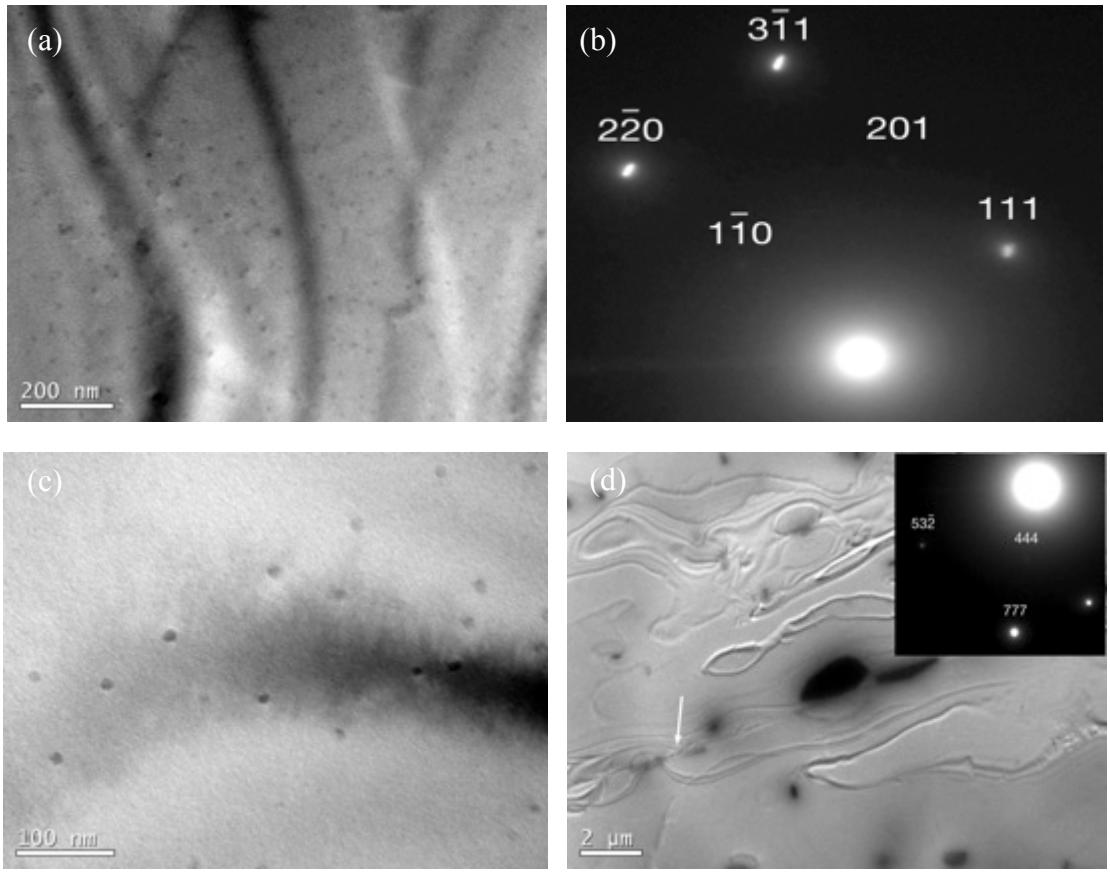

Figure 2. Bright-field micrographs of (a) Al_3Zr $L1_2$ precipitates, (b) SADP of Fig.2a, (c) Al_3Zr $L1_2$ precipitates with higher magnification and (d) β-Al_3Mg_2 precipitates.

Figure 3 show TEM micrographs of the Al-0.9Mg-0.2Zr alloy aged at 650 K for 100 h. Fig.3a is a bright-field image, where it is possible to observe β precipitates, some of them interacting with dislocations. Fig.3b is the complementary dark-field image of Fig.3a, using (200) reflections from the SADP in the bottom right of the image. It shows a large number density of finer Al_3Zr precipitates (small white dots). The "rod-like" precipitates indicated by arrows are also Al_3Zr $L1_2$ spherical particles that formed near each other along dislocations (Ness, 1972); (Knipling, 2006).

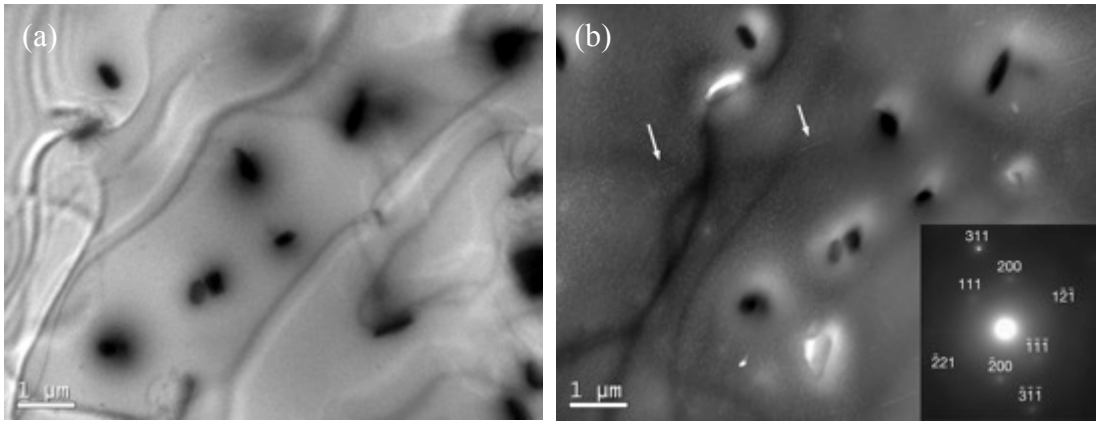

Figure 3. (a) Bright-field micrograph and (b) complementary dark-field image of Fig.3a of sample aged at 650 K for 100 h.

3.3. Strengthening mechanisms

During aging, as the particles nucleate and grow, there are different active strengthening mechanisms, depending if the particles are shearable by dislocations or not (Lefebvre et al., 2014); (Kendig and Miracle, 2002), (Marquis et al., 2003); (Ardell, 1985). The Al_3Zr $L1_2$ precipitates are shearable for $\langle r \rangle < 3$ nm (Lefebvre et al., 2014), were mechanisms such as order strengthening, modulus hardening and coherency strengthening are competitive (Knipling et al., 2010); (Lefebvre et al., 2014); (Marquis et al., 2003). For greater $\langle r \rangle$ values, precipitates are bypassed by dislocations and thus, hardened by the Orowan dislocation looping mechanism (Lefebvre et al., 2014), (Knipling et al. 2010). Kendig and Miracle (2002) found that in $Al_3(Sc,Zr)$ $L1_2$ precipitates, the shearing to bypassing transition occurs at 20 to 25 nm. As the Al_3Zr particles in this study present $\langle r \rangle = 8$ nm, Orowan dislocation looping mechanism will be considered.

Though there are not studies indicating whether β particles are shearable or not, such present a lattice parameter – a much greater than Al: $a_{Al} = 4.0495$ Å (Zedalis and Fine, 1983), $a_{\beta} = 28.239$ Å (Samson, 1965), indicating a large mismatch with Al, therefore in the interaction between β particles and dislocations the Orowan mechanism is considered.

The increase in strength due to the Orowan mechanism ($\Delta\sigma_{ow}$) is defined in Eq. (1) (Embury, 1989), where M =3.06 is the Taylor factor for the matrix (Frost and Ashby, 1982a), G = 25.4 GPa is the Al shear modulus, b = 0.286 nm the Burgers vector (Frost and Ashby, 1982b), $\nu = 0.345$ the Poisson ratio (Meyers and Chawla, 2009) and L is the effective interparticle spacing (Eq. (2)) (Ardell, 1985), where f is the equilibrium volume fraction of precipitates at a given temperature, determined using the lever rule.

$$\Delta\sigma_{ow} = M \cdot \left(0.4Gb/\pi(1-\nu)^{\frac{1}{2}}\right) \cdot ln\left(\frac{2\langle r \rangle}{b}\right) \cdot L^{-1} \quad (1)$$

$$L = \langle r \rangle\left(\sqrt{2\pi/3f} - \pi/2\right) \quad (2)$$

Using the measured $\langle r \rangle$ values, the increase in strength due to precipitation hardening is calculated using the Pythagorean addition rule (Eq. (3)) (Ardell, 1985), where $\Delta\sigma_p$ is the increase in strength due to precipitation hardening, $\Delta\sigma_{ow}^{Al_3Zr}$ the contribution of the Al_3Zr particles, $\Delta\sigma_{ow}^{\beta}$ the contribution of the β particles, η_1 and η_2, the proportion of Al_3Zr and β particles, respectively. The experimental and theoretical results are shown in Tab. 2 (together with other values that are going to be explained further in the text), were e_i is the difference between the experimental and theoretical results. The experimental results for precipitation hardening were taken as the difference between the microhardness values of samples aged at 650 K for 100 h and as cast, converted to MPa using a conversion chart (Knipling, 2006) and multiplied by 1/3 (Tabor, 1956) to convert from microhardness to strength (in MPa).

$$\Delta\sigma_p{}^2 = \left(\Delta\sigma_{ow}^{Al_3Zr}\right)^2\eta_1 + \left(\Delta\sigma_{ow}^{\beta}\right)^2\eta_2 \quad (3)$$

The increase in strength due to solid solution is defined in Eq. (4), were ε = 3.8E-07 MPa is a proportionality constant for Al-Mg alloys (Kendig and Miracle, 2002), and c is the Mg concentration (in at.%). Results are given in Tab. 2. The experimental $\Delta\sigma_{ss}$ is taken as the difference between the as cast microhardness of the Al-0.9Mg-0.2Zr alloy and an Al-0.2Zr alloy. The values were converted to strength (in MPa) likewise described for the precipitation hardening values.

$$\Delta\sigma_{ss} = 3.1\varepsilon G c^{1/2}/700 \quad (4)$$

Table 2, shows the results of each strengthening contribution. Although the difference between the experimental and theoretical results for $\Delta\sigma_{ss}$ is low, the magnitude of e_i for $\Delta\sigma_p$ is comparatively high. However, these values must not be evaluated separately, because the individual contributions of each mechanism should be corrected. The superposition of the strengthening mechanisms – $\Delta\sigma_t$, is determined using the empirical relation in Eq. (5) (Lagerpusch et al., 2001); (Ardell, 1985), where n is an adjustable parameter between 1 and 2 (Lagerpusch et al., 2001). While some authors adopted n = 1 (Cabibbo, 2013); (Qiao et al., 2011). Other authors, such as Marquis et al. (2002), that studied the influence of precipitation hardening by Al_3Sc $L1_2$ particles and solid solution hardening by Mg in an Al-2Mg-0.2Sc alloy adopted n = 2. Ardell (1985) explains that if the matrix is pure, linear superposition (n = 1) must be obtained, once the critical resolver shear stress of the matrix is not obstacle controlled. Lagerpusch et al. (2001), on the other hand, explained that in some alloys the lattice and/or modulus mismatch of the precipitates can lead to inconsistencies with the linear approach. The authors found an n ~ 1.8 for Cu alloys strengthened by SiO_2 particles and Au solid solution.

In Table 2, the e_i value for $\Delta\sigma_t$ with n = 2 is -2.3 MPa, indicating goodness of fit. If n = 1 is adopted, the magnitude of e_i increases to – 31.0 MPa. Marquis et al. (2003) suggests that the linear superposition is the upper bound of the increase in strength and, thus, n = 2 is the lower bound.

$$\Delta\sigma_t{}^n = \Delta\sigma_{ss}{}^n + \Delta\sigma_p{}^n \quad (5)$$

Table 2. Experimental and theoretical results for the increase in strength due to the studied mechanisms.

Component	Increase in strength (MPa)		e_i (MPa)
	Experimental	Theoretical	
$\Delta\sigma_{ss}$	45.4 ± 3.6	42.7	2.7
$\Delta\sigma_p$	24.5 ± 5.9	58.2	-33.7
$\Delta\sigma_t{}^{(1)}$	69.9 ± 9.5	72.2	-2.3

(1): for n = 2

4. CONCLUSIONS

After isothermal aging at 650 K for 100 h, the alloy presented the peak strength condition, with an increase in strength of 24.5 MPa, from the as cast condition. After aging at 650 K for 400h, the alloy presented overaging, and strength decreased to the as cast levels. The increase in strength due to solid solution hardening is 45.4 MPa. At 700 K, the nucleation of precipitates was hindered and no appreciable increase in strength was observed.

During microstructural characterization it was possible to observe a high number density of homogeneously distributed nanometer-scale $\langle r \rangle$ = 8 nm Al_3Zr precipitates and a lower number density of plate-like β particles with $\langle r \rangle$=235 nm.

The contributions to strengthening of both solid solution and precipitation hardening were calculated. The theoretical contributions presented good agreement with the experimental results of samples aged at 650 K for 100h, when using an addition factor of n = 2.

5. ACKNOWLEDGEMENTS

The authors would like to thank CAPES for the scholarship, CNPq for the financial support and LCME/UFSC by the training for the operation of the TEM.

6. REFERENCES

Ardell, A.J., 1985, “Precipitation Hardening”, Metallurgical Transactions A, Vol.16A, pp. 2131-2165.

Cabibbo, M., 2013, “Microstructure strengthening mechanisms in an Al-Mg-Si-Sc-Zr equal channel angular pressed aluminum alloy”, Applied Surface Science, Vol.281, pp. 38-43.

Embury, J.D., Lloyd, D.J., Ramachandran, T.R., 1989, “Strengthening Mechanisms in Aluminum Alloys”, In: Vasudevan, A.K., Doherty, R.D. “Aluminum Alloys – Contemporary Research and Applications”. Ed. Academic Press. São Diego, Estados Unidos, pp.579-604.

Hatch, J.E., 1984, “Constitution of Alloys”, In: Hatch, J.E., “Aluminum: Properties and Physical Metallurgy”. Ed. American Society for Metals, Metals Park, pp. 25-57.

Frost, H.J., Ashby, M.F., 1982a, “The F.C.C. Metals; Ni, Cu, Ag, Al, Pb and γ-Fe”, in: “Deformation-Mechanism Maps: The Plasticity and Creep of Metals and Ceramics”, 6 Out. 2015, <http://engineering.dartmouth.edu/defmech/>.

Frost, H.J., Ashby, M.F., 1982b, “Rate-Equations”, In: Frost, H.J., Ashby, M.F. “Deformation-Mechanism Maps: The Plasticity and Creep of Metals and Ceramics”, 6 Out. 2015, <http://engineering.dartmouth.edu/defmech/>.

Kendig, K.L., Miracle, D.B., 2002, “Strengthening mechanisms of an Al-Mg-Sc-Zr alloy”, Acta Materialia, Vol.50, pp. 4165-4175.

Knipling, K.E., 2006, “Development of a Nanoscale Precipitation-Strengthened Creep-Resistant Aluminum Alloy Containing Trialuminide Precipitates”, Tese de doutorado, Universidade Northwestern, Evanston, IL, Estados Unidos, pp. 1-241.

Knipling, K.E., Dunand, D.C., Seidman, D.N., 2006, “Criteria for developing castable, creep-resistant aluminum-based alloys – A review”, *Zeitschrift fuer Metallkunde,* Vol.97, No.3, pp. 246-265.

Knipling, K.E., Dunand, D.C. and Seidman, D.N., 2007, “Nucleation and Precipitation Strengthening in Dilute Al-Ti and Al-Zr Alloys”, Metallurgical and Materials Transactions A, Vol.38A, pp. 2522-2563.

Knipling, K. E., Karnesky, R.A., Lee, C.P., Dunand, D.C., Seidman, D.N., 2010, “Precipitation evolution in Al-0.1Sc, Al-0.1Zr, and Al-0.1Sc-0.1Zr (at.%) alloys during isochronal aging”. Acta Materialia, Vol.58, pp. 5184-5195.

Kumar, K.S., 1990, “Ternary intermetallics in aluminum-refractory metal-X systems (X=V, Cr, Mn, Fe, Co, Ni, Cu, Zn)”, International Materials Reviews, Vol.35, No.6, pp. 293-327.

Lagerpusch, U., Mohles, V., Nembach, E., 2001, “On the additivity of solid solution and dispersion strengthening” Materials Science and Engineering A, 319-321, pp. 176-178.

Lefebvre, W., Masquelier, N., Houard, J., Patte, R., Zapolsky, H., 2014, "Tracking the path of dislocations across ordered Al_3Zr nano-precipitates in three dimensions". Scripta Materialia, Vol.70, pp. 43-46.

Marquis, E.A., Seidman, D. N. and Dunand, D. C., 2003, "Effect of Mg addition on the creep and yield behavior of an Al-Sc alloy", Acta Materialia, Vol.51, pp.4751-4760.

Meyers, M.A., Chawla, K.K., 2009, "Creep and Superplasticity", In: "Mechanical Behavior of Materials". Ed. Cambridge University Press, pp.653-712.

Ness, E., 1972, "Precipitation of the metastable cubic Al_3Zr-phase in subperitectic Al-Zr alloys", Acta Metallurgica, Vol. 20, pp. 499-506.

Qiao, X.Q., Gao, N., Starink, M., 2012, "A model of grain refinement and strengthening of Al Alloys due to col severe plastic deformation", Philosophical Magazine, Vol.92, No.4, pp.446-470.

Robson, J.D., Prangnell, P.B., 2003, "Modelling Al_3Zr dispersoind precipitation in multicomponent aluminium alloys", Materials Science and Engineering A, Vol.352, pp. 240-250.

Samson, S., 1965, "The crystal structure of the phase β Mg_2Al_3", Acta Crystallopraphica, Vol.19, pp. 401-413.

Sanders, R.E., Baumann, S.F., Stumpf, H.C., 1989, "Wrought Non-Heat-Treatable Aluminum Alloys", In: Vasudevan, A.K., Doherty, R.D. "Aluminum Alloys – Contemporary Research and Applications". Ed. Academic Press, São Diego, Estados Unidos, pp. 66-108.

Tabor, D., 1956, "The physical meaning of indentation and scratch hardness", British Journal of Applied Physics Vol.7, pp.159-166.

Wu, H., Wen, S.P., Gao, K.Y., Huang, H., Wang, W., Nie, Z.R., 2014, "Effect of Er additions on the precipitation strengthening of Al-Hf alloys", Scripta Materialia, Vol.87, pp. 5-8.

Zhang, Y., Gao, K., Wen, S., Huang, H., Nie, Z. and Zhou, D., 2014, "The study on the coarsening process and precipitation strengthening of Al_3Er precipitate in Al-Er binary alloy", Journal of Alloys and Compounds, Vol.610, p.27-34.

Zedalis, M.S., Fine, M.E., 1983, "Lattice parameter variation of Al_3(Ti, V, Zr, Hf) in Al-2at.% (Ti, V, Zr, Hf) alloys. Scripta Metallurgica, Vol.17, pp. 1247-1251.

Zedalis, M.S., Fine, M.E., 1986, "Precipitation and Ostwald Rippening in Dilute Al Base-Zr-V Alloys", Metallurgical Transactions A, Vol.17A, pp. 2187-2198.

7. RESPONSIBILITY NOTICE

The authors, Pedro Henrique Lamarão Souza, Carlos Augusto Silva de Oliveira and José Maria do Vale Quaresma are the only responsible for the printed material included in this paper.